Electronic Supplementary Material (ESI) for Dalton Transactions.
This journal is © The Royal Society of Chemistry 2017

Electronic Supplementary Information

for the

Manuscript Entitled

Hydroxide-bridged dicopper complexes: Influence of secondary coordination sphere on structure and catecholase activity

Deepak Bansal and Rajeev Gupta*

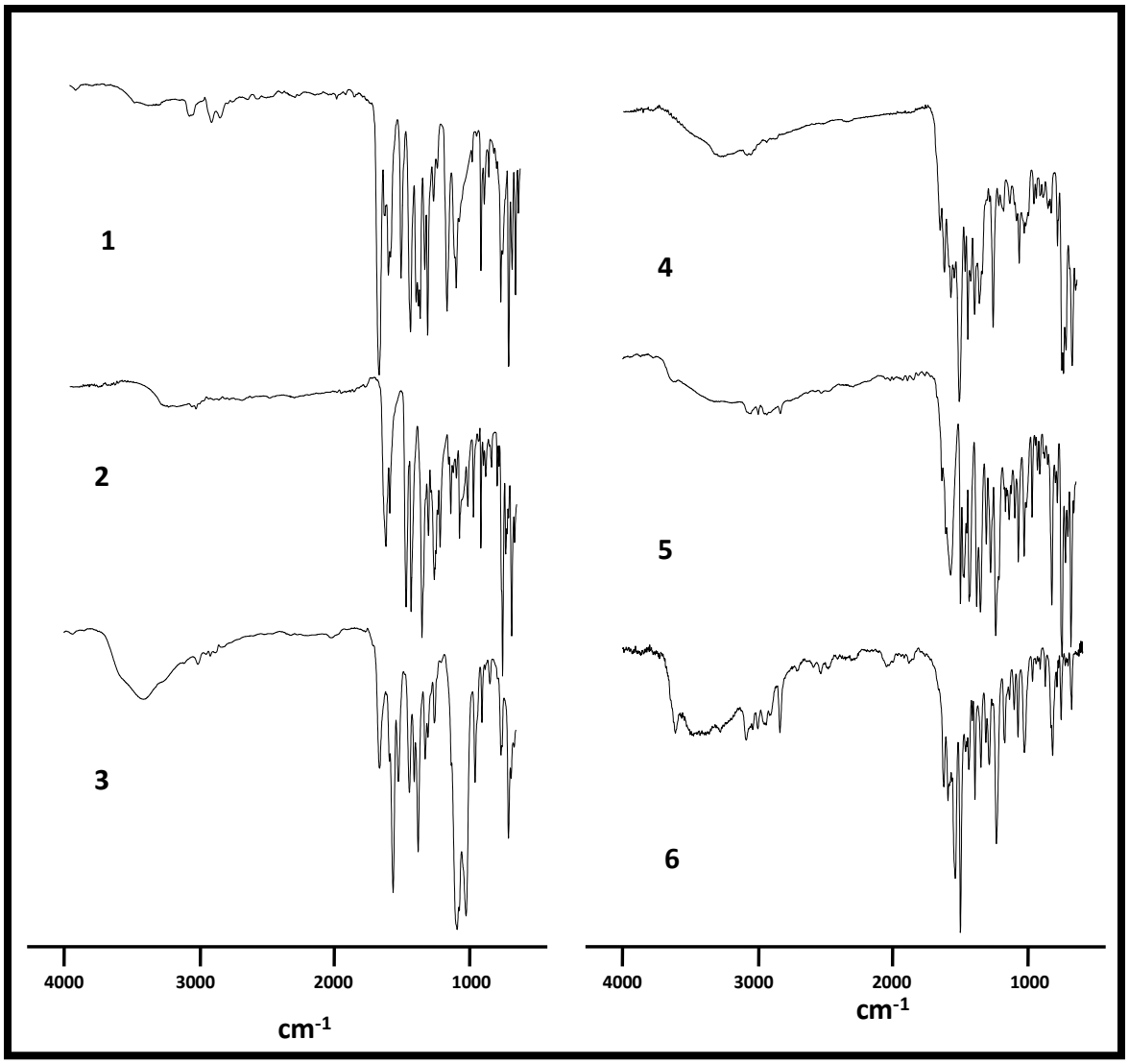

Figure S1. FTIR spectra of complexes **1**-**6**.

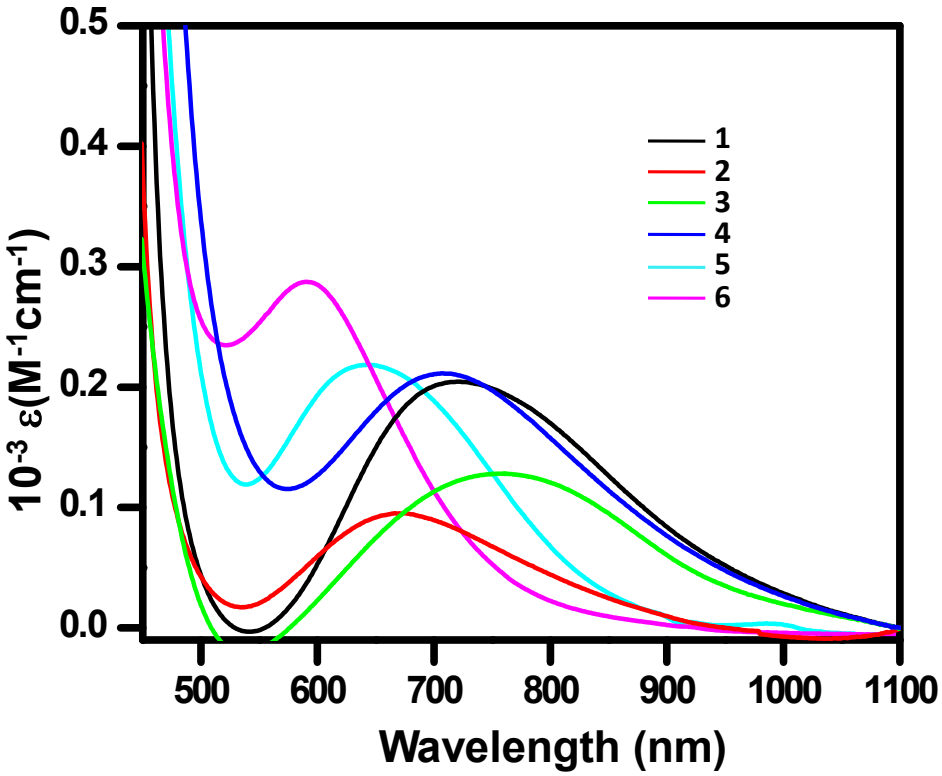

Figure S2. Absorption spectra of complexes **1-6** recorded in DMF solvent.

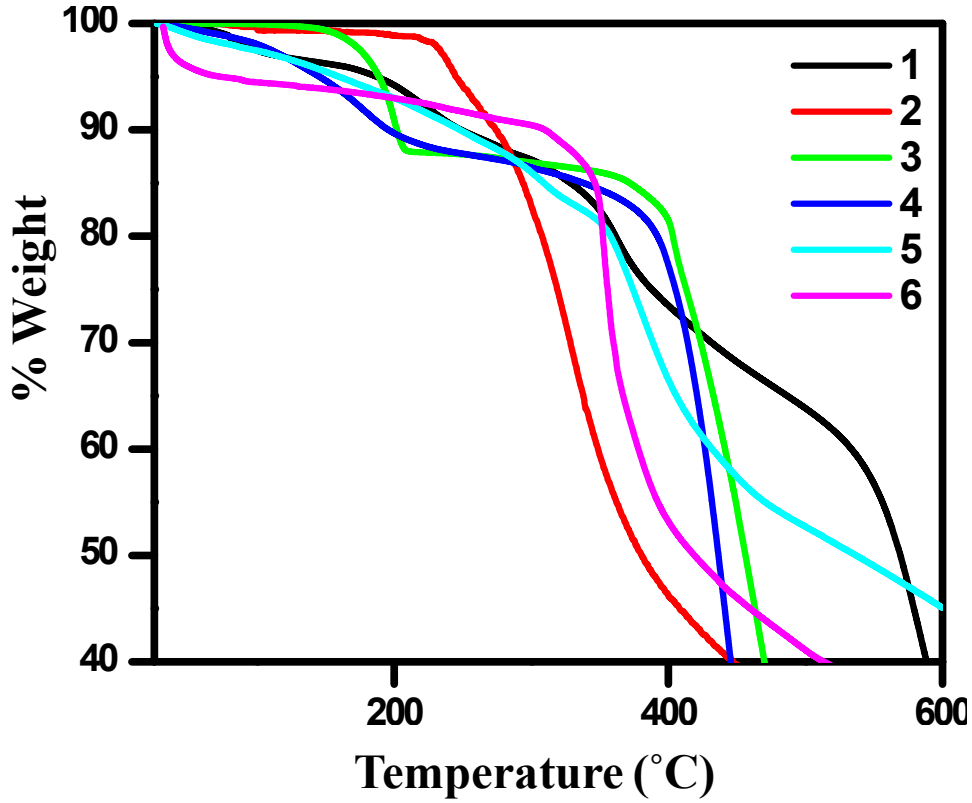

Figure S3. Thermal Gravimetric Analysis (TGA) plots for complexes **1-6**.

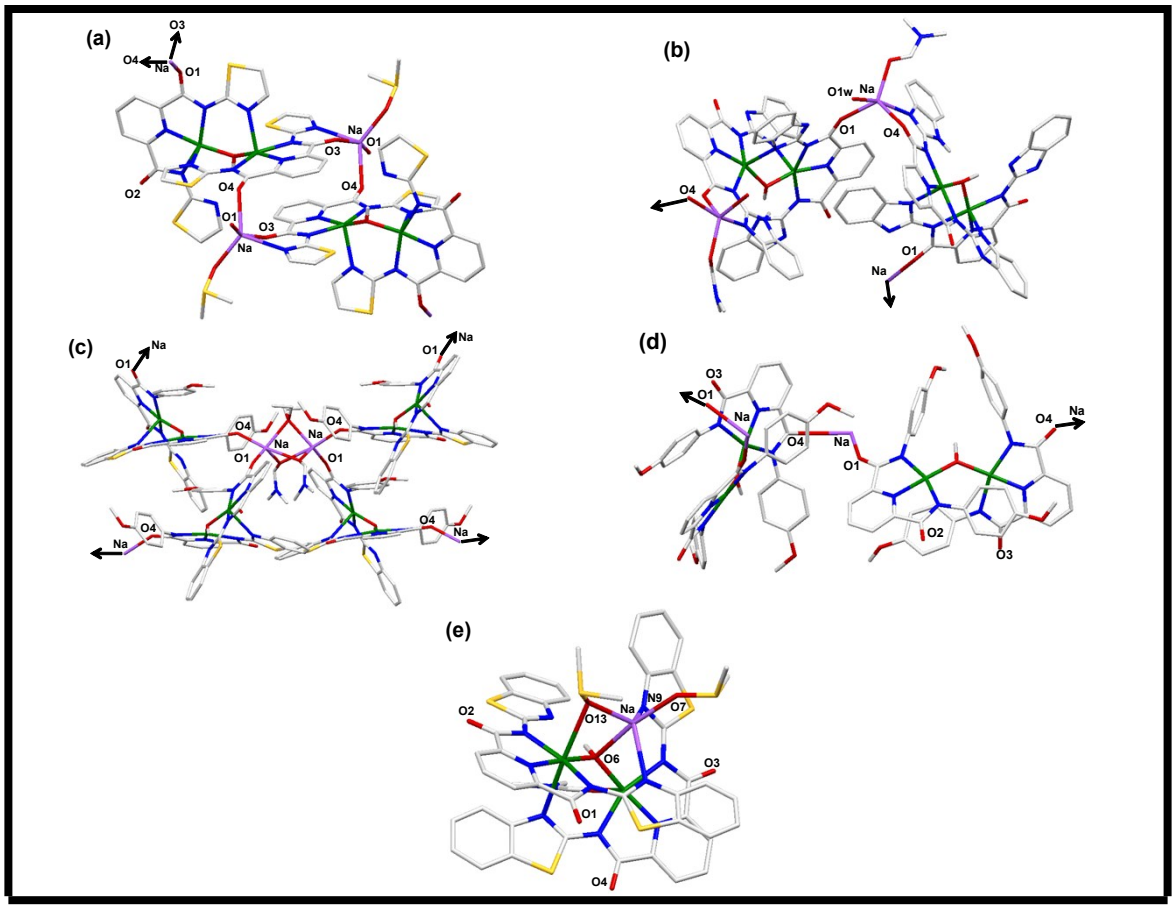

Figure S4. Crystal structures of complexes **1** (a), **2** (e), **4** (b), **5** (c) and **6** (d) displaying the coordination of complex anion with the sodium ion.

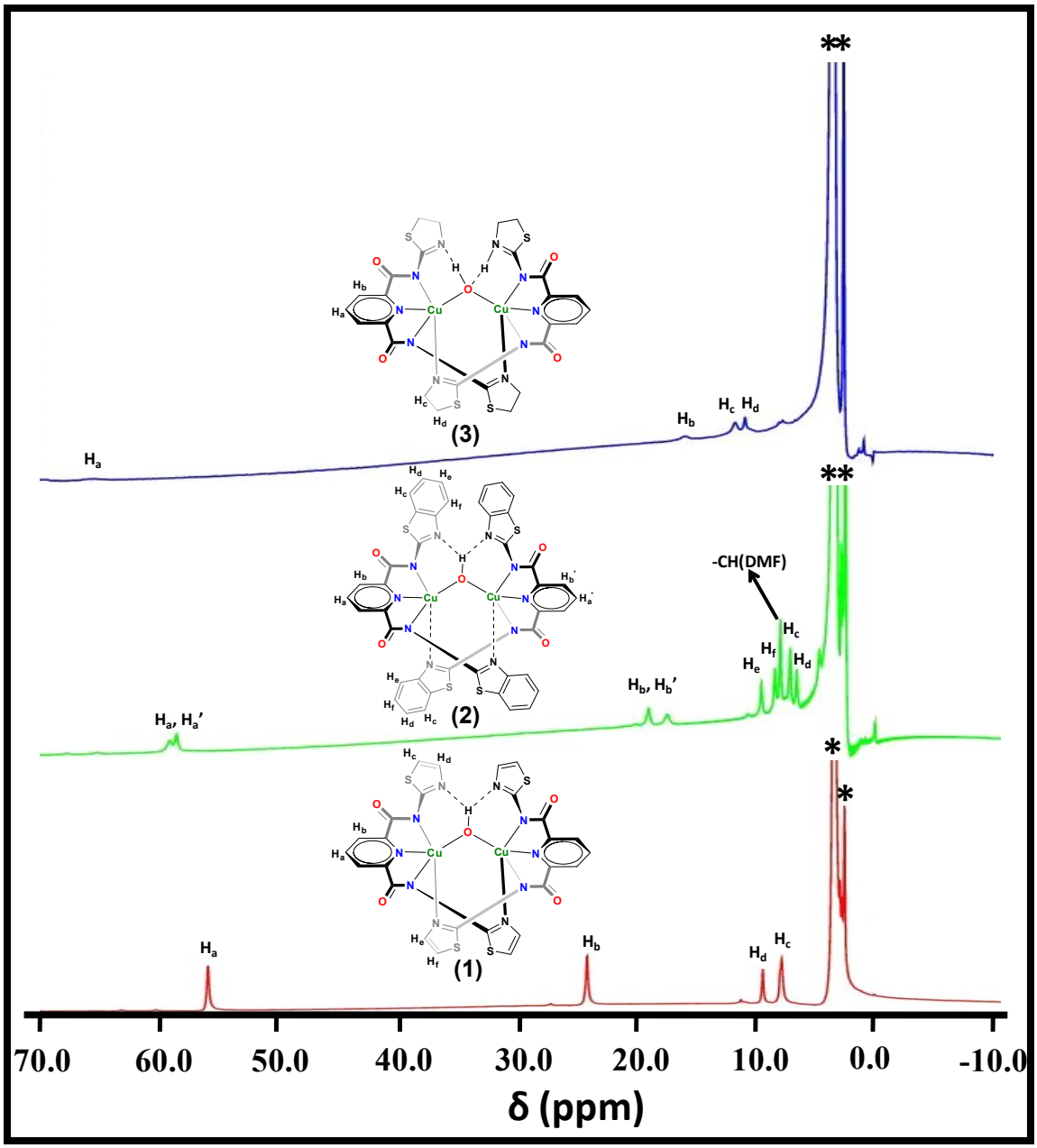

Figure S5. ^{1}H NMR spectra of complexes **1-3** in d_6-DMSO; * represents the residual solvent and H_2O peak, respectively.

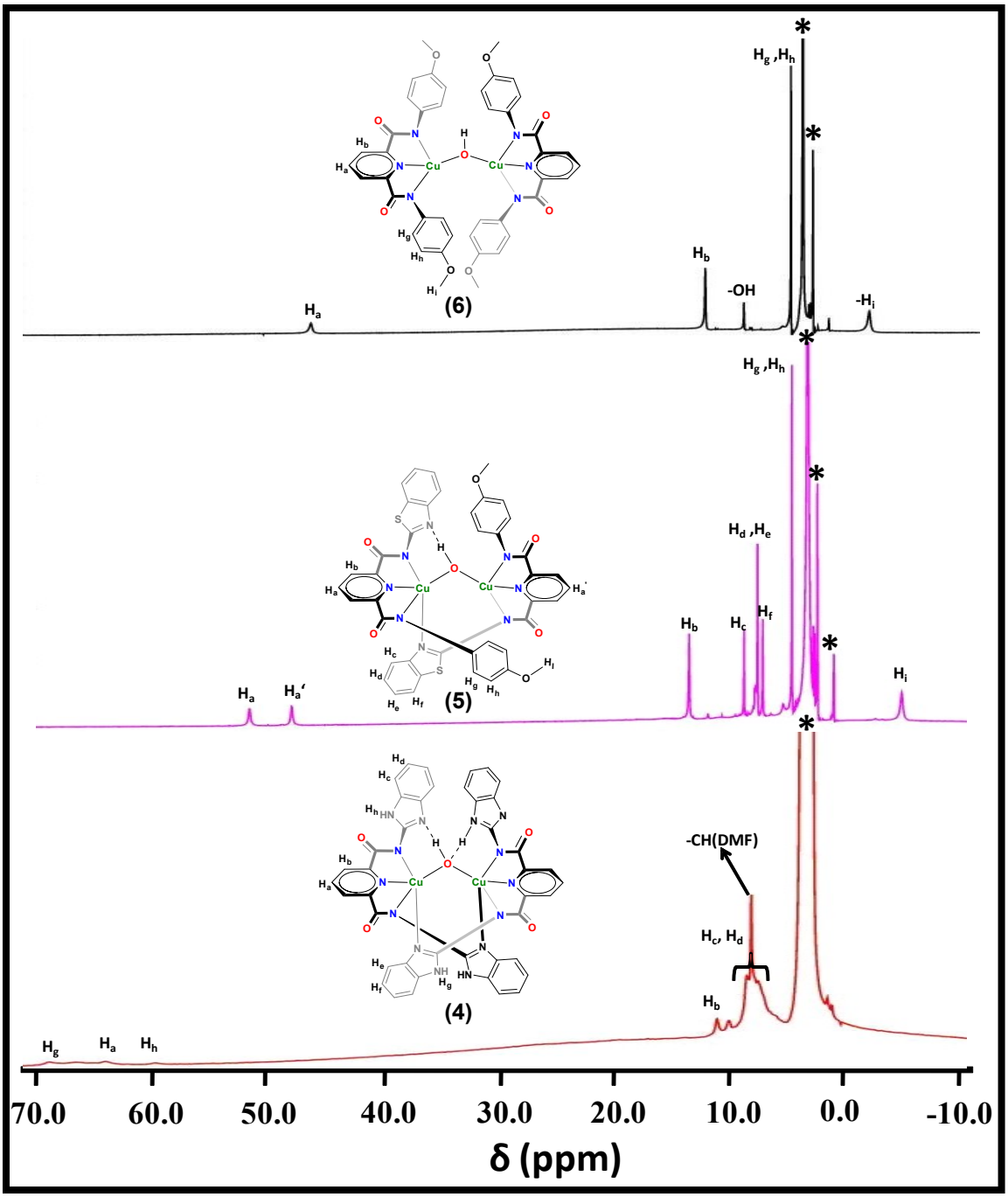

Figure S6. ^{1}H NMR spectra of complexes **4-6** in d_6-DMSO; * represents the residual solvent and H_2O peak, respectively.

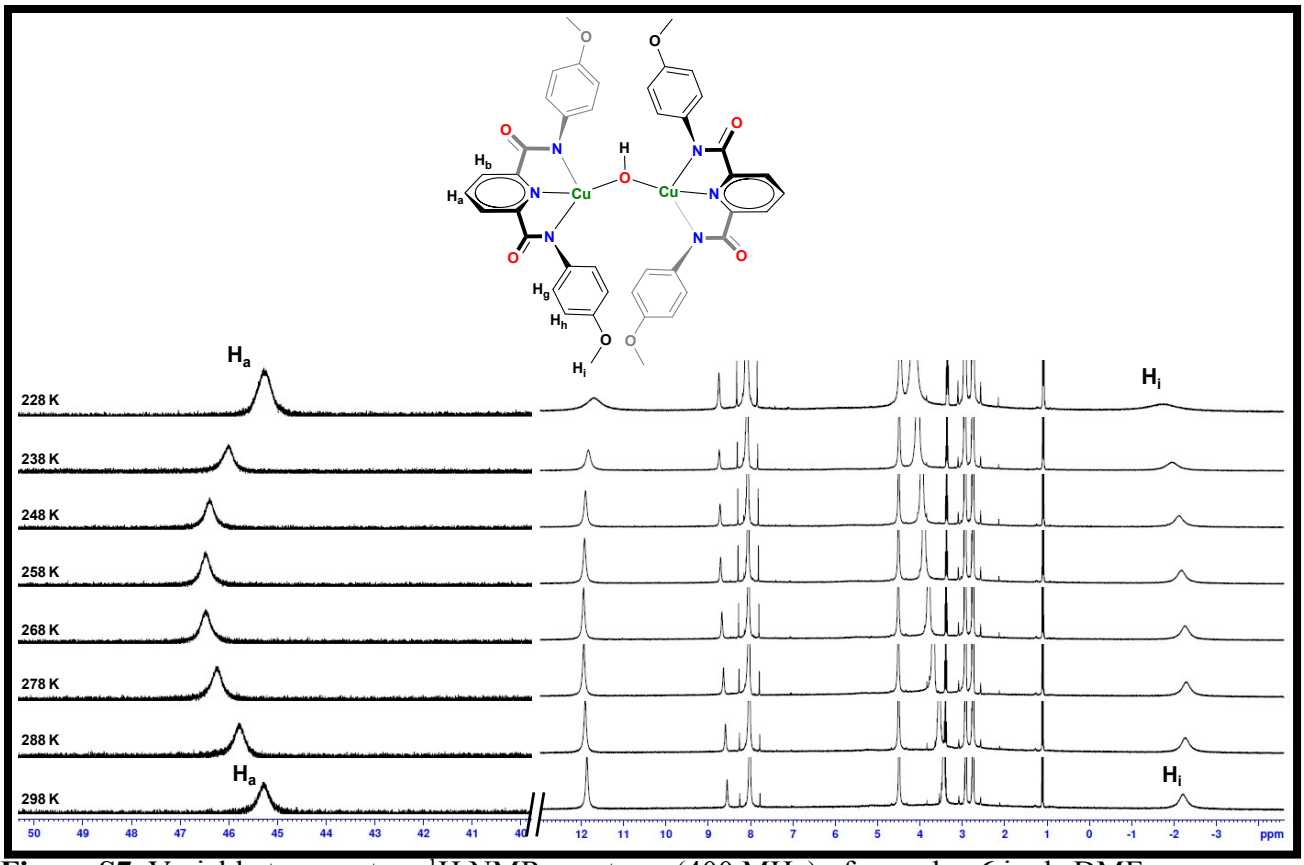

Figure S7. Variable temperature ^{1}H NMR spectrum (400 MHz) of complex **6** in d_7-DMF.

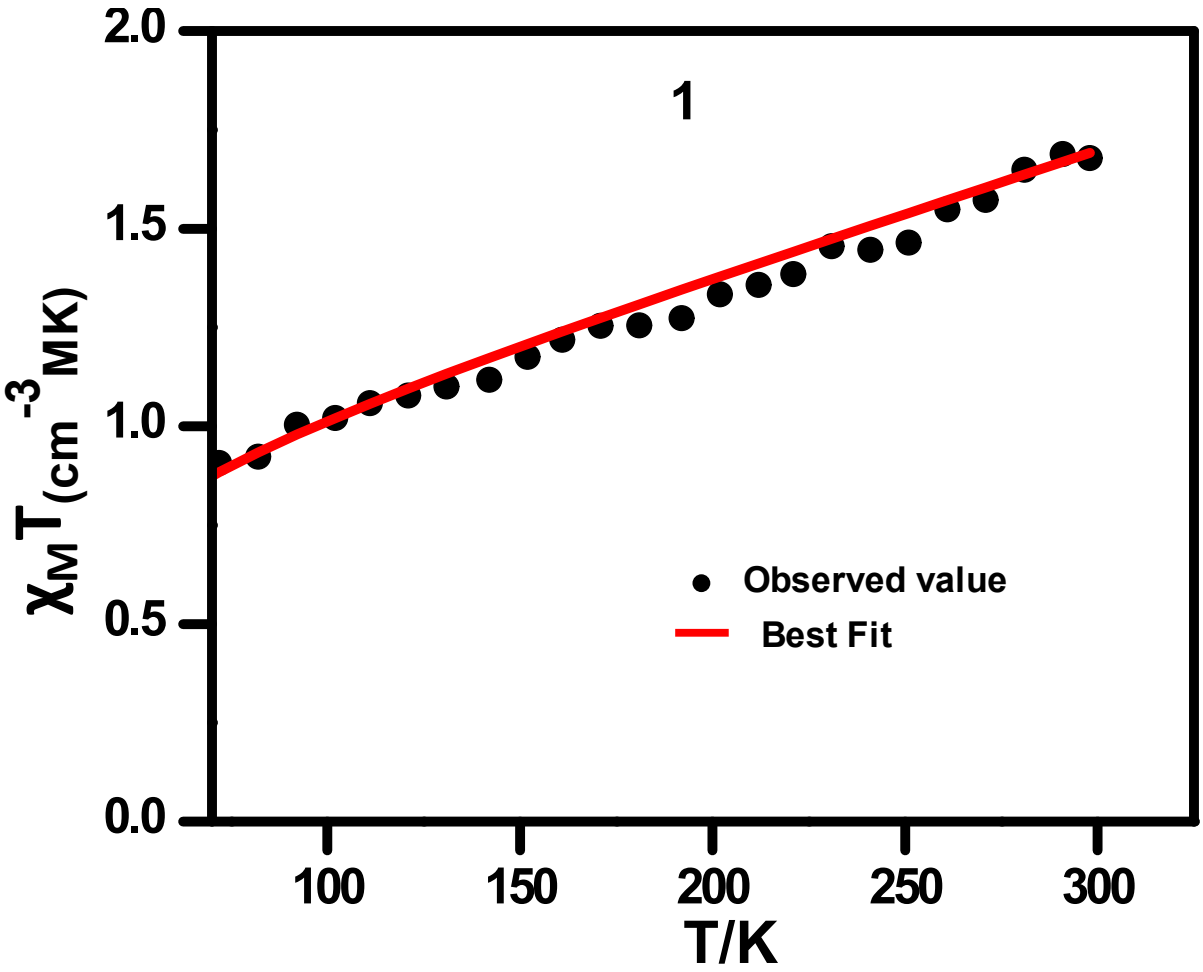

Figure S8. Temperature dependence of the product $\chi_M T$ for complex **1**. The black spheres are the experimentally observed data whereas the red line is the fit to the experimental data as described in the text.

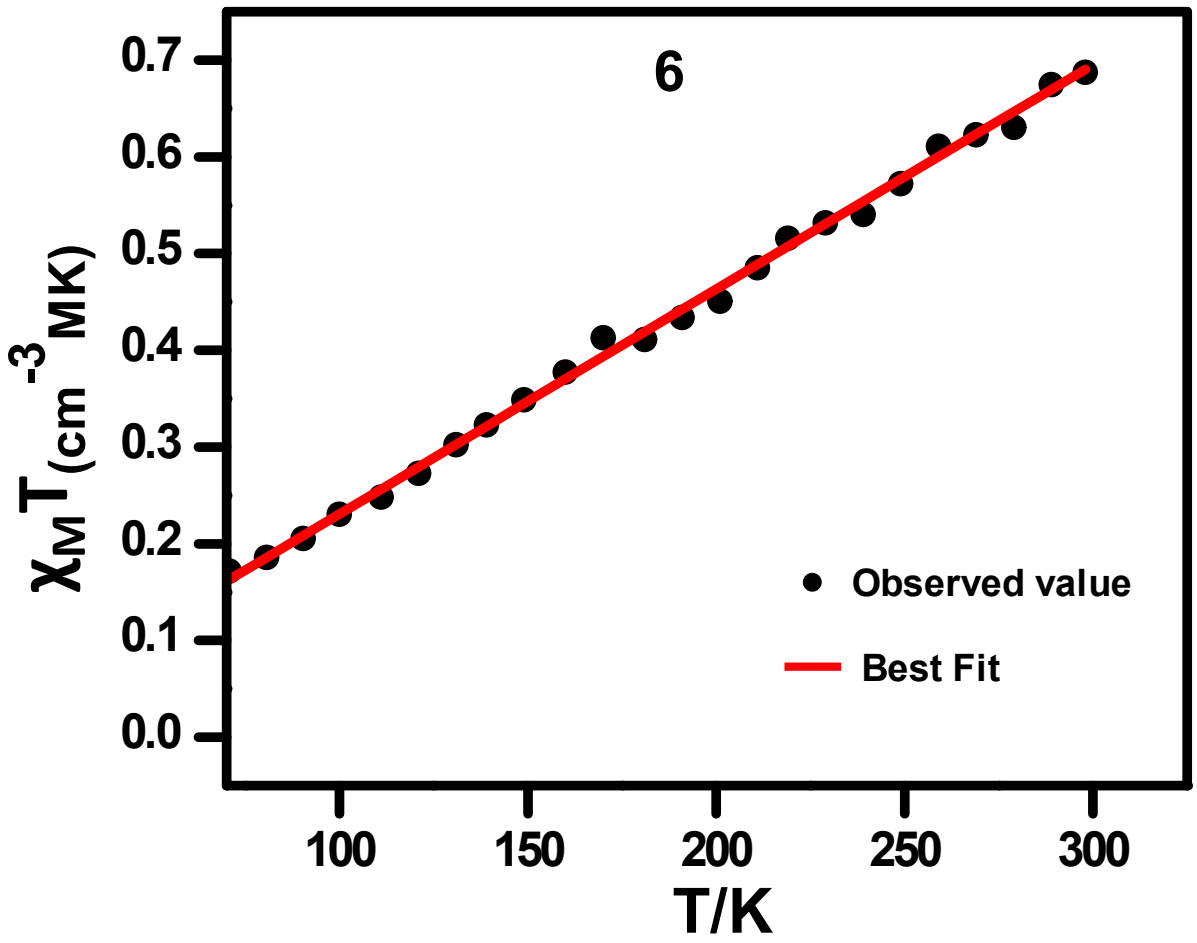

Figure S9. Temperature dependence of the product $\chi_M T$ for complex **6**. The black spheres are the experimentally observed data whereas the red line is the fit to the experimental data as described in the text.

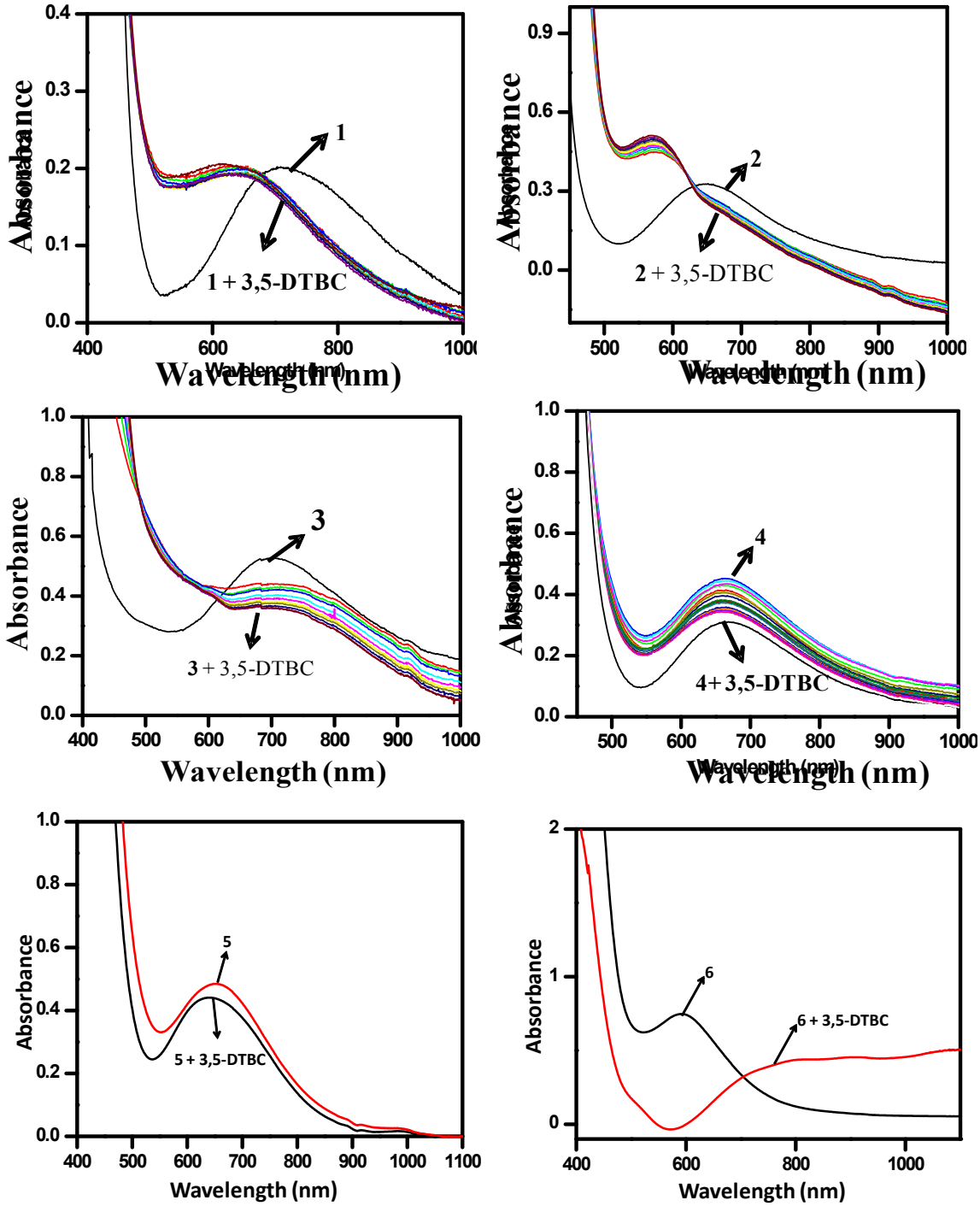

Figure S10. Change in absorbance of complexes **1-6** after the addition of 100 equiv. of 3,5-ditertbutyl catechol in DMSO solution.

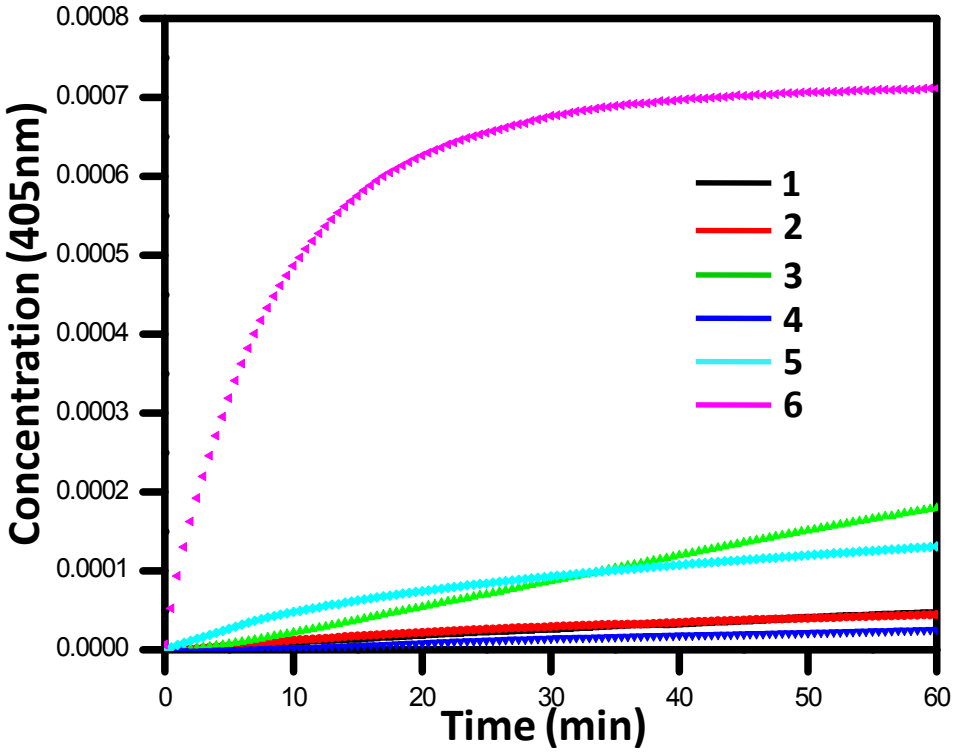

Figure S11. Time-dependent monitoring of change in concentration at 405 nm due to formation of 3,5-DTBQ in presence of complexes **1**-**6**.

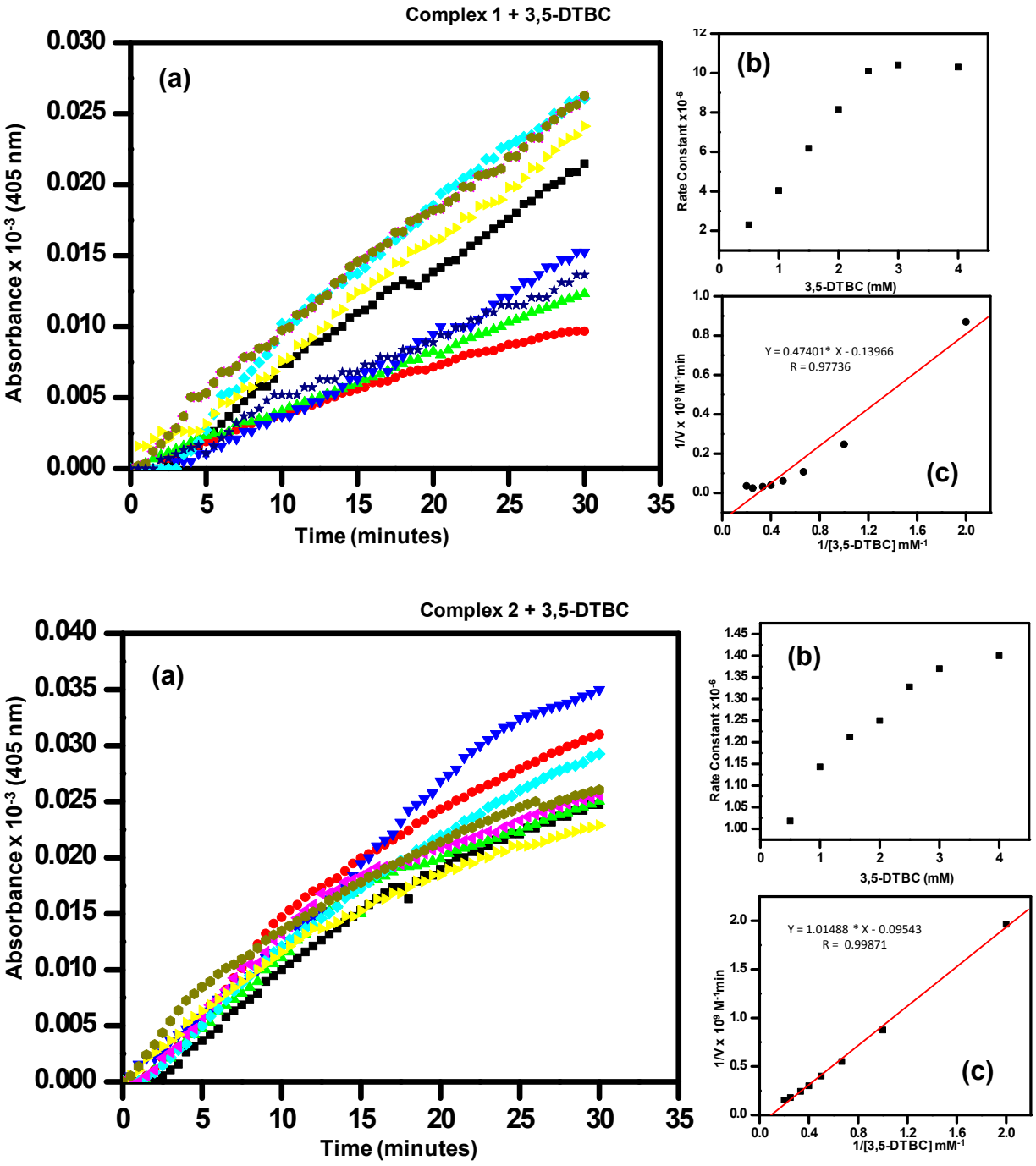

Figure S12 (a) Time dependent monitoring of change in absorbance at 405 nm due to formation of 3,5-DTBQ in presence of complex **1** (above) and **2** (below) in DMSO-MeOH mixture (Conditions: complex = 25 μM; 3,5-DTBC = 0.5-5.0 mM; oxygen saturated 5% DMSO-MeOH (v/v) solution; Temp = 303 K). (b) Plot between rate constant w.r.t. different concentrations of 3,5-DTBC. (c) Lineweaver-Burk plot between 1/V and 1/[S].

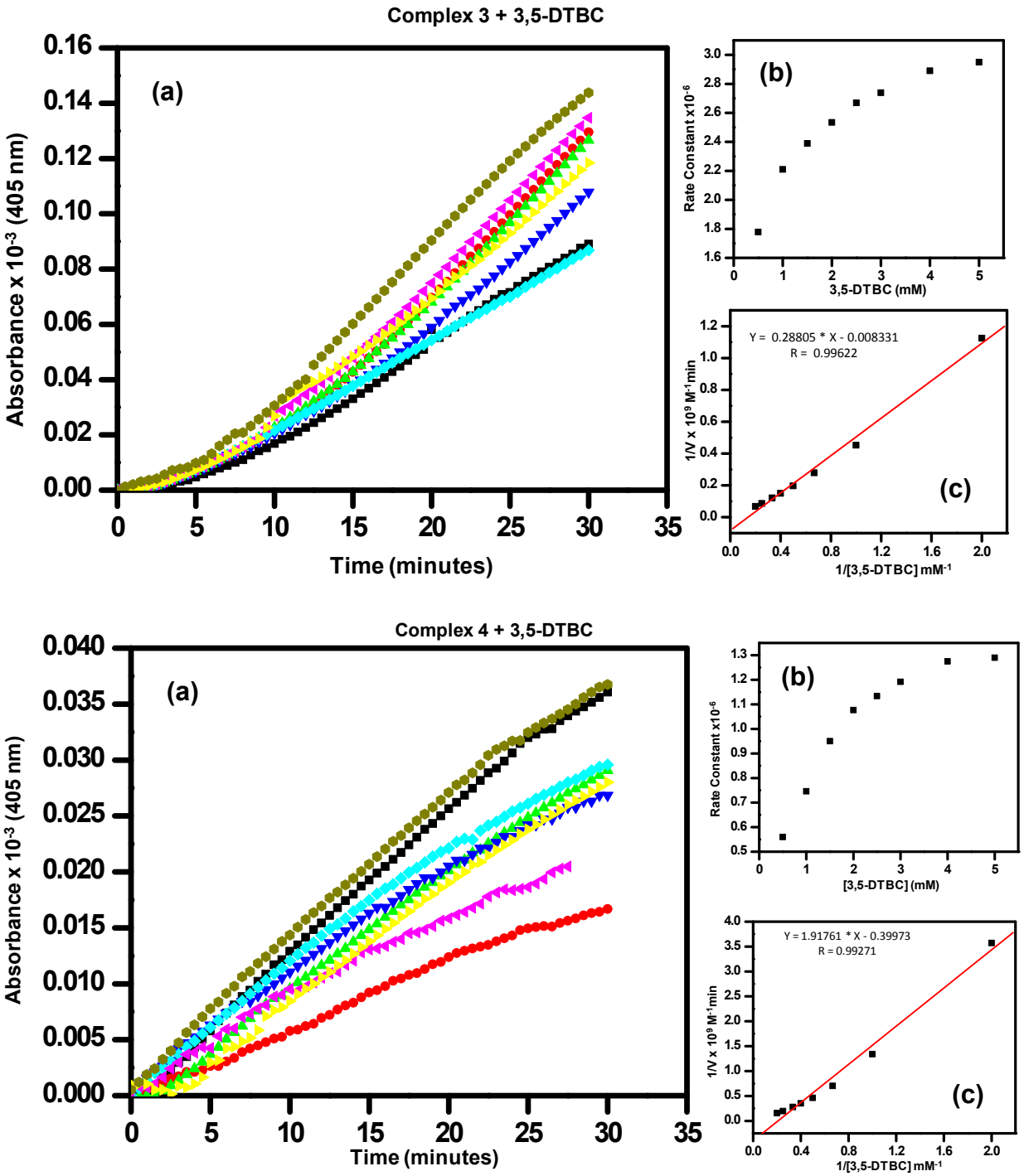

Figure S13. (a) Time dependent monitoring of change in absorbance at 405 nm due to formation of 3,5-DTBQ in presence of complex **3** (above) and **4** (below) in DMSO-MeOH mixture (Conditions: complex = 25 μM; 3,5-DTBC = 0.5-5.0 mM; oxygen saturated 5% DMSO-MeOH (v/v) solution; Temp = 303 K). (b) Plot between rate constant w.r.t. different concentrations of 3,5-DTBC. (c) Lineweaver-Burk plot between 1/V and 1/[S].

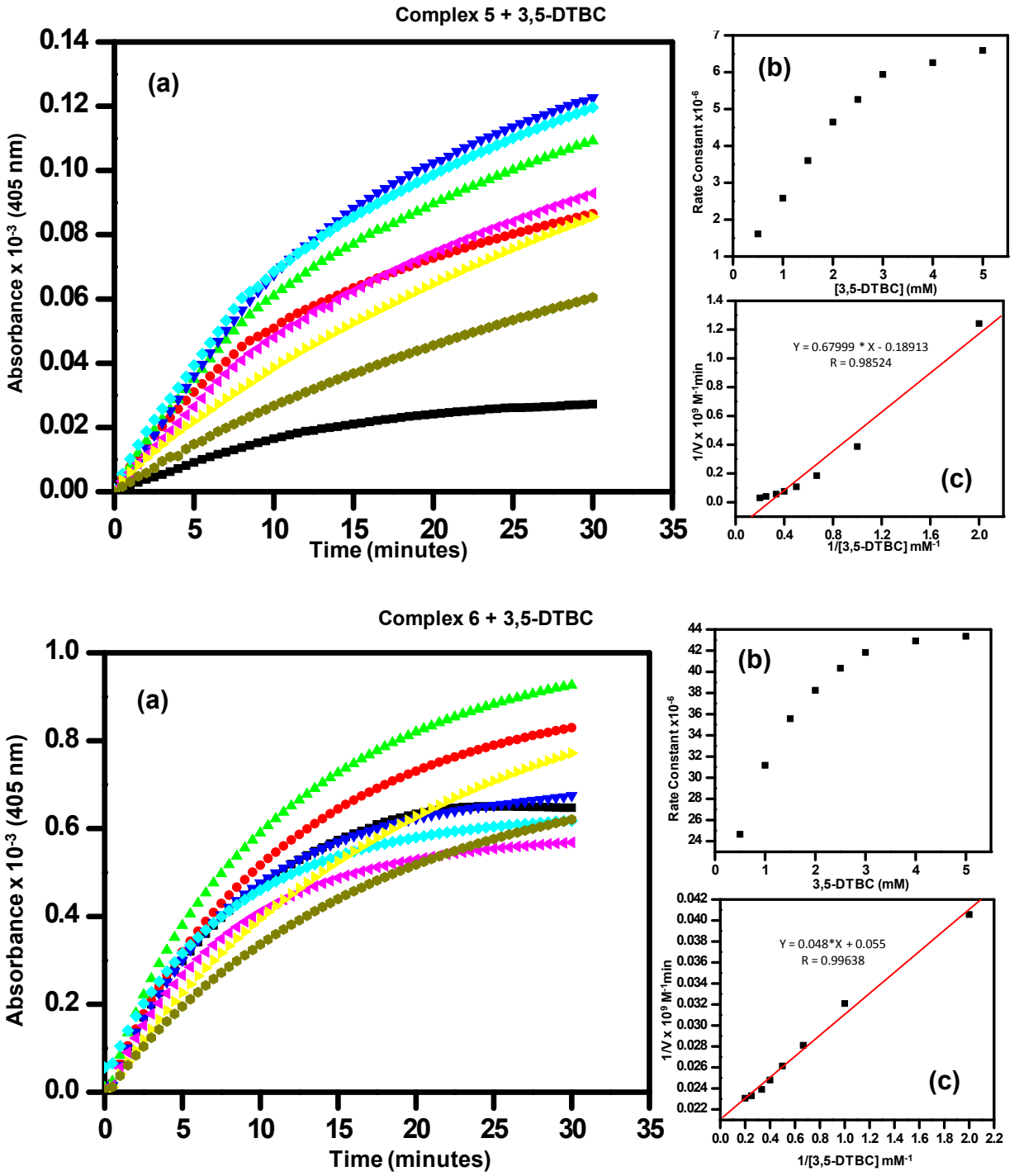

Figure S14. (a) Time dependent monitoring of change in absorbance at 405 nm due to formation of 3,5-DTBQ in presence of complex **5** (above) and **6** (below) in DMSO-MeOH mixture (Conditions: complex = 25 μM; 3,5-DTBC = 0.5-5.0 mM; oxygen saturated 5% DMSO-MeOH (v/v) solution; Temp = 303 K). (b) Plot between rate constant w.r.t. different concentrations of 3,5-DTBC. (c) Lineweaver-Burk plot between 1/V and 1/[S].

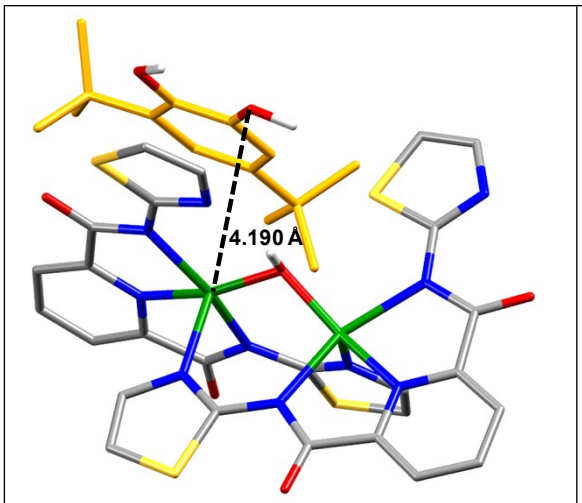

1 + 3,5-DTBC

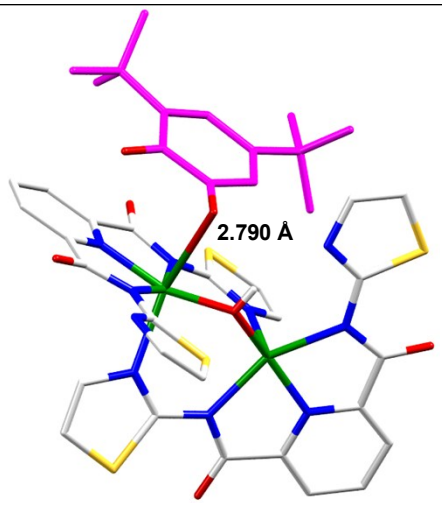

1 + 3,5-DTBQ

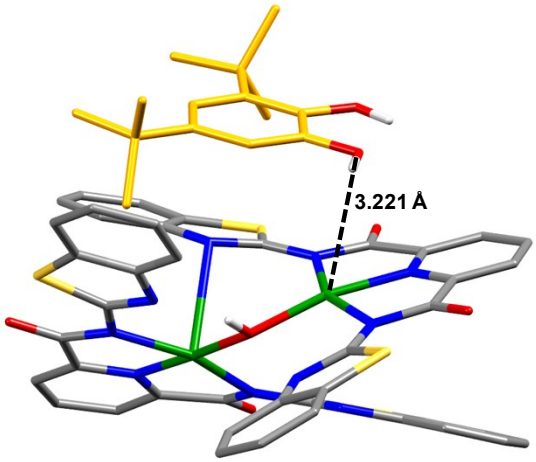

2 + 3,5-DTBC

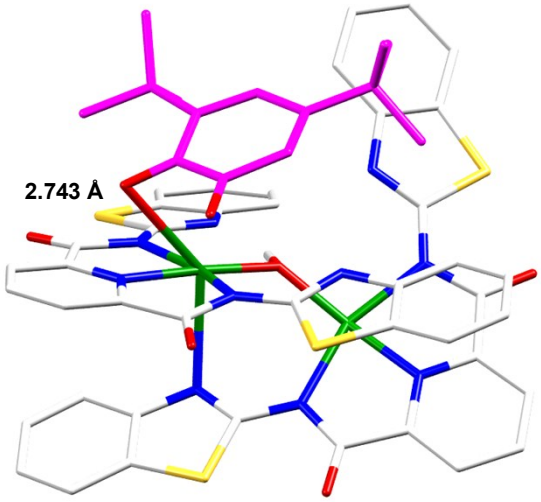

2 + 3,5-DTBQ

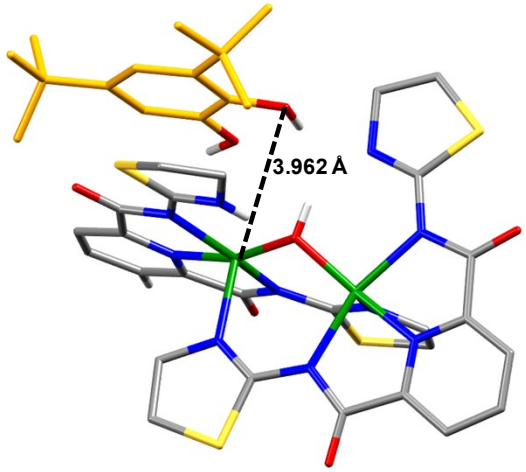

3 + 3,5-DTBC

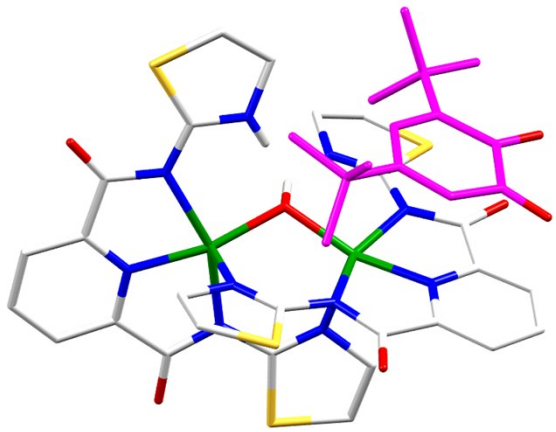

3 + 3,5-DTBQ

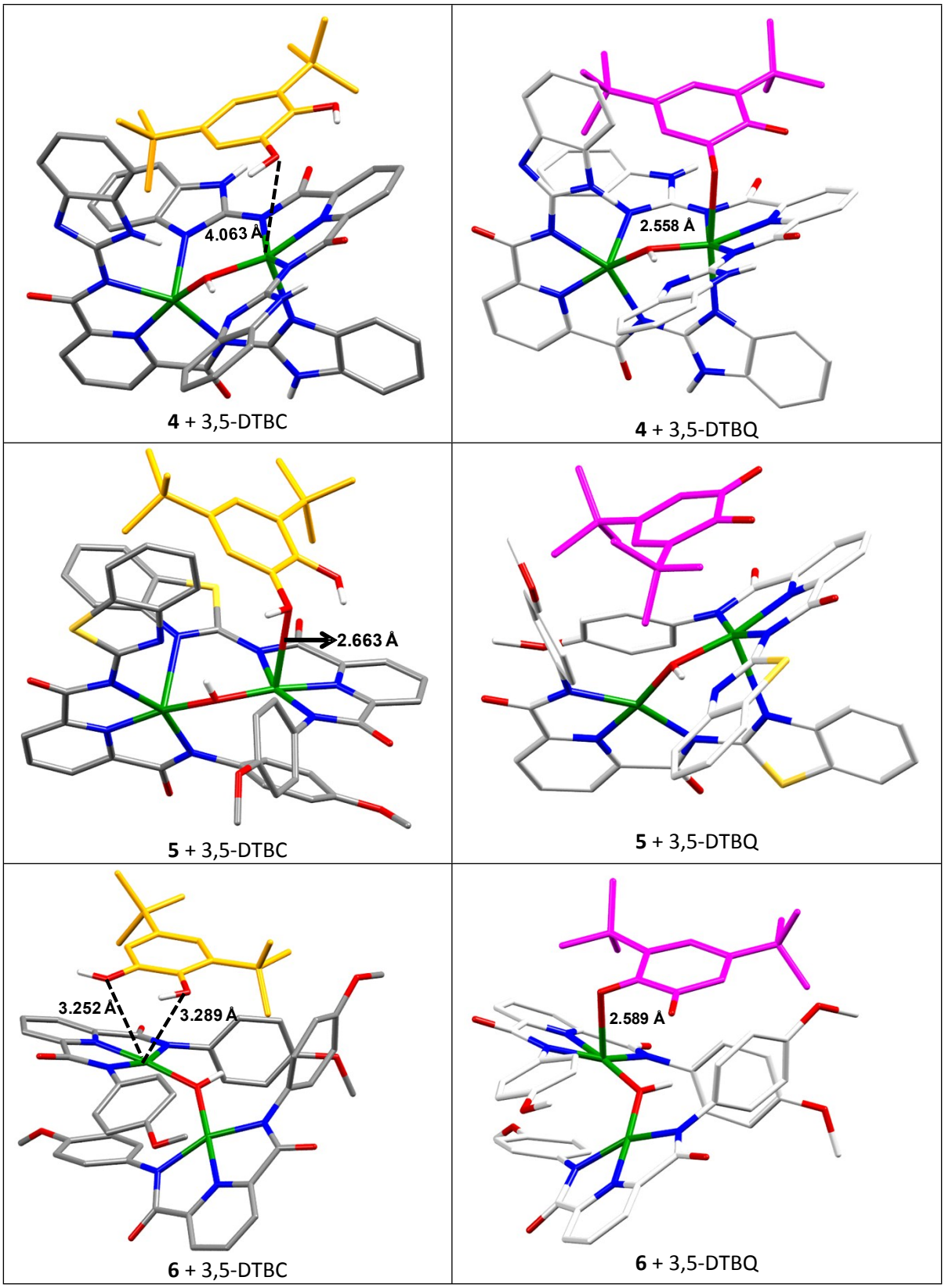

Figure S15. Docked structures of complexes **1-6** with 3,5-DTBC (left column) and 3,5-DTBQ (right column).

Table S1. Selected bond distances (Å) and angles (°) for complexes **1**-**5**.

Bond	**1**	**2**	**3**	**4**	**Bond**	**5**
Cu1-N1	2.113(3)	2.096(5)	2.085(4)	2.163(5)	Cu1-N1	2.007(7)
Cu1-N2	1.942(3)	1.924(5)	1.936(4)	1.943(5)	Cu1-N2	1.967(7)
Cu1-N3	2.100(3)	2.093(5)	2.043(4)	2.117(5)	Cu1-N3	2.038(7)
Cu1-N10	2.196(3)	2.245(4)	2.675	2.198(5)	Cu1-N9	2.427(6)
Cu1-O6	1.890(2)	1.896(3)	1.890(3)	1.919(4)	Cu1-O7	1.922(6)
Cu2-N5	2.218(3)	2.191(4)	2.815	2.263(5)	Cu2-N7	1.894(7)
Cu2-N8	2.159(3)	2.126(4)	2.131(4)	2.136(5)	Cu2-N6	2.022(6)
Cu2-N7	1.940(3)	1.934(4)	1.943(4)	1.939(5)	Cu2-N8	2.068(7)
Cu2-N6	2.122(3)	2.099(4)	2.114(4)	2.100(5)	Cu2-O7	1.833(6)
Cu2-O6	1.888(2)	1.912(3)	1.886(3)	1.915(5)	-------	-------
Cu2-O6-Cu1	117.60(13)	115.62(17)	129.28(18)	117.8(2)	Cu2-O7-Cu1	124.6(3)
O6-Cu1-N2	164.99(12)	163.35(18)	176.75(16)	160.9(2)	O7-Cu1-N2	169.7(3)
O6-Cu1-N3	98.26(11)	96.37(18)	101.17(16)	95.2(2)	O7-Cu1-N1	99.5(3)
N2-Cu1-N3	79.02(11)	79.6(2)	79.68(19)	79.2(2)	N2-Cu1-N1	80.2(3)
O6-Cu1-N1	101.33(11)	101.61(16)	99.49(16)	102.2(2)	O7-Cu1-N9	89.7(2)
N2-Cu1-N1	78.56(11)	79.6(2)	79.84(19)	78.1(2)	N2-Cu1-N9	100.6(3)
N3-Cu1-N1	156.21(11)	158.07(19)	159.17(18)	153.9(2)	N1-Cu1-N9	98.5(3)
O6-Cu1-N10	98.48(11)	96.44(15)	-------	95.4(2)	N3-Cu1-N9	92.5(3)
N2-Cu1-N10	96.48(11)	100.07(19)	-------	103.6(2)	O7-Cu2-N7	173.2(3)
N3-Cu1-N10	95.32(11)	96.96(17)	-------	103.2(2)	O7-Cu2-N6	100.5(3)
N1-Cu1-N10	95.02(11)	93.42(17)	-------	94.4(2)	N7-Cu2-N6	76.8(3)
O6-Cu2-N7	161.72(12)	162.72(16)	166.77(16)	163.4(2)	O7-Cu2-N8	99.3(3)
O6-Cu2-N6	99.62(11)	105.04(15)	99.59(15)	101.3(2)	N7-Cu2-N8	83.9(3)
N7-Cu2-N6	79.36(11)	80.05(16)	79.21(17)	79.6(2)	N6-Cu2-N8	159.6(3)

O6-Cu2-N8	100.07(11)	94.48(15)	101.88(15)	97.71(19)	O7-Cu1-N3	100.9(3)
N7-Cu2-N8	78.01(11)	77.63(17)	78.78(17)	78.1(2)	N2-Cu1-N3	77.8(3)
N6-Cu2-N8	156.67(11)	156.62(17)	157.99(16)	156.2(2)	N1-Cu1-N3	156.8(3)
O6-Cu2-N5	94.33(11)	94.39(15)	------	94.0(2)	------	------
N7-Cu2-N5	103.78(11)	101.42(16)	------	102.3(2)	------	------
N6-Cu2-N5	101.58(10)	97.21(16)	------	98.5(2)	------	------
N8-Cu2-N5	89.30(10)	93.94(17)	------	94.4(2)	------	------

Table S2. Crystallographic data collection and structure solution parameters for complexes **1** - **3**.

	1•2DMSO	**2•2DMSO•2DMF**	**3•DMSO•H_2O**
Chem. Formula	$C_{30}H_{27}Cu_2N_{10}NaO_7S_6$	$C_{52}H_{49}Cu_2N_{12}NaO_9S_6$	$C_{28}H_{32}Cu_2N_{10}O_7S_5$
Formula weight	982.0	1328.48	908.02
Temp (K)	293(2)	293(2)	293(2)
Crystal System	Triclinic	Monoclinic	Triclinic
Space group	*P* -1	*P* 2_1/n	*P* -1
a [Å]	11.7066(7)	11.8275(7)	11.4773(10)
b [Å]	12.6984(10)	13.7942(7)	21.5497(9)
c [Å]	13.6077(10)	37.139(2)	14.462(9)
α [°]	71.836(7)	90	104.578(6)
β [°]	85.232(5)	91.374(5)	108.957(7)
γ [°]	81.455(6)	90	91.628(7)
V [Å^3]	1899.3(2)	6057.5(6)	1892.8(2)
d [g cm^{-3}]	1.717	1.457	1.593
μ [mm^{-1}]	1.522	0.981	1.457
F(000)	996	2728	928
R(*int*)	0.0310	0.0552	0.0281
Final *R* indices [I>2σ(I)][a]	R_1 = 0.0409 wR_2 = 0.1020	R_1 = 0.0712 wR_2= 0.1730	R_1 = 0.0590 wR_2 = 0.1733
R indices (all data)	R_1 = 0.0480 wR_2 = 0.1071	R_1 = 0.0881 wR_2 = 0.1840	R_1 = 0.0744 wR_2 = 0.1863
GOF (F^2)	1.034	1.111	1.056

[a] $R_1 = \Sigma||F_o|-|F_c||/\Sigma|F_o|$; $wR = \{[\Sigma(|F_o|^2|F_c|^2)^2]\}^{1/2}$

Table S3. Crystallographic data collection and structure refinement parameters for complexes **4** and **5**.

	4•2DMF•DMSO•2H$_2$O	**5•DMF•C$_4$H$_8$O**
Chem. Formula	$C_{50}H_{51}Cu_2N_{16}NaO_{10}S$	$C_{94}H_{82}Cu_4N_{18}Na_2O_{17}S_4$
Formula weight	1218.20	2164.16
Temp (K)	293	293
Crystal System	Monoclinic	Monoclinic
Space group	$P\,2_1/c$	C_2/c
a [Å]	13.3647(8)	25.553(5)
b [Å]	13.9486(7)	13.374(5)
c [Å]	28.7657(16)	28.901(4)
α [°]	90	90
β [°]	101.93(5)	109.122(13)
γ [°]	90	90
V [Å^3]	5246.6(5)	9332(4)
d [g cm^{-3}]	1.542	1.540
μ [mm^{-1}]	0.934	1.077
F(000)	2512	4440
R(*int*)	8958 [0.1061]	8213 [0.3193]
Final R indices [I>2σ(I)][a]	R_1 = 0.0853, wR_2 = 0.1988	R_1 = 0.1120, wR_2 = 0.2490
R indices (all data)	R_1 = 0.1305, wR_2 = 0.2244	R_1 = 0.1824, wR_2 = 0.3131
GOF (F^2)	1.032	1.003

[a] $R_1 = \Sigma||F_o|-|F_c||/\ \Sigma|F_o|$; $wR = \{[\Sigma(|F_o|^2|F_c|^2)^2]\}^{1/2}$